



Swansea University  
Prifysgol Abertawe



## Cronfa - Swansea University Open Access Repository

---

This is an author produced version of a paper published in :

*Biotechnology Journal*

Cronfa URL for this paper:

<http://cronfa.swan.ac.uk/Record/cronfa32940>

---

### Paper:

James, S., Hilal, N. & Wright, C. (2017). Atomic force microscopy studies of bioprocess engineering surfaces - imaging, interactions and mechanical properties mediating bacterial adhesion. *Biotechnology Journal*, 1600698  
<http://dx.doi.org/10.1002/biot.201600698>

---

This article is brought to you by Swansea University. Any person downloading material is agreeing to abide by the terms of the repository licence. Authors are personally responsible for adhering to publisher restrictions or conditions. When uploading content they are required to comply with their publisher agreement and the SHERPA RoMEO database to judge whether or not it is copyright safe to add this version of the paper to this repository.

<http://www.swansea.ac.uk/iss/researchsupport/cronfa-support/>

1  
2  
3  
4  
5  
6  
7  
8  
9  
10  
11  
12  
13  
14  
15  
16  
17  
18  
19  
20  
21  
22  
23  
24  
25  
26  
27  
28  
29  
30  
31  
32

Review

**Title: Atomic Force Microscopy Studies of Bioprocess Engineering Surfaces – Imaging, Interactions and Mechanical Properties Mediating Bacterial Adhesion.**

Sean A James<sup>1</sup>  
Nidal Hilal<sup>2</sup>  
Chris J Wright<sup>1</sup>

1. Biomaterials, Biofouling and Biofilms Engineering Laboratory (B<sup>3</sup>EL, System and Process Engineering Center, College of Engineering, Swansea University, Fabian Way, Swansea SA1 8EN, UK.
2. Centre for Water Advanced Technologies and Environmental Research (CWATER), College of Engineering, Swansea University, Fabian Way, Swansea SA1 8EN, UK

**Correspondence:** Chris J Wright, System and Process Engineering Center, Swansea University Bay Campus, Fabian Way, SA1 8EN, Swansea, Wales.

**E-mail:** C.J.Wright@swansea.ac.uk

**Keywords:** Atomic force microscopy, Bacteria, Biofouling, Force measurement, Nanoindentation.

**Abbreviations:** **DVLO**, Derjaguin, Landau, Verwey, Overbeek theory; **XDVLO**, Extended Derjaguin, Landau, Verwey, Overbeek theory; **EPS**, Extracellular Polymeric Substance; **LB-EPS**, Loosly Bound Extracellular Polymeric Substance; **TB-EPS**, Tightly Bound Extracellular Polymeric Substance; **SMFS**, Single Molecule Force Spectroscopy; **SCFS**, Single Cell Force Spectroscopy.

1 **Abstract**

2 The detrimental effect of bacterial biofilms on process engineering surfaces is well documented.  
3 Thus, interest in the early stages of bacterial biofilm formation; in particular bacterial adhesion  
4 and the production of anti-fouling coatings has grown exponentially as a field. During this time,  
5 Atomic force microscopy (AFM) has emerged as a critical tool on the evaluation of bacterial  
6 adhesion. Due to its versatility AFM offers not only insight into the topographical landscape and  
7 mechanical properties of the engineering surfaces, but elucidates, through direct quantification  
8 the topographical and biomechanical properties of the foulants The aim of this review is to  
9 collate the current research on bacterial adhesion, both theoretical and practical, and outline  
10 how AFM as a technique is uniquely equipped to provide further insight into the nanoscale  
11 world at the bioprocess engineering surface. .

12

1  
2  
3  
4  
5  
6  
7  
8  
9  
10  
11  
12  
13  
14  
15  
16  
17  
18  
19  
20  
21  
22  
23  
24  
25  
26  
27  
28  
29  
30  
31  
32  
33  
34  
35  
36  
37  
38  
39

**1 Introduction**

Bacterial contamination of water based industrial infrastructure is unavoidable, consequently, the formation of bacterial biofilm on process engineering surfaces is a substantial issue for many industrial processes. A bacterial biofilm consists of a heterogeneous consortium of sessile organisms embedded within a gel like support matrix formed from exopolysaccharides, proteins, and extracellular DNA, typically adhered to a solid support structure. The formation of a biofilm offers bacteria considerable advantages over the planktonic state, including a higher concentration of nutrients and aqueous gasses, increased proximity to other cells, and protection from biocidal, chemical and biological attack. Additionally, biofilm formation is known to result in numerous detrimental effects on process engineering infrastructure, including reduction in the efficacy of cooling towers, heat exchangers, ion exchangers and, filtration membranes, as well as causing a substantial level of end product spoilage. The combined fiscal impact of bacterial bioburden is likely to amount to many millions, if not billions of pounds of lost income due to reductions in process efficiency and repairs. Biofilms are of particular concern as the innate resistance offered by the structure often result in removal being almost impossible, while simultaneously facilitating the re-contamination of any downstream infrastructure that may have been successfully cleaned.

Several control strategies are often employed in an effort to control bacterial biofouling, typically this will involve the use of toxic chemical such as sodium hypochlorite, glutaraldehyde, isothiazoline, and chlorine dosing. However, these strategies are non-specific, damaging to infrastructure and often ineffective in the removal of fully established biofilms. Furthermore, tightening of legislation on the use of antimicrobials has further limited their efficacy, therefore highlighting the need for the implementation of new strategies. As bacterial adhesion marks the initiation of biofilm formation the creation novel anti-adhesion compounds and coatings offers promising solutions to the biofouling problem. Typically, these compounds and coatings alter surface chemistry therefore modifying the strength of binding forces facilitating bacterial adhesion. Hence furthering our understanding of the fundamental bacterial substrate interactions that promote primary adhesion is essential, as the application of such knowledge is paramount in the formation and design of these strategies (1–3). Despite this, development of such technologies is limited primarily due to the lack of understanding of the forces governing these interactions. Theoretical models predicting the interactions between bacteria and substrates are well established, with comprehensive modeling of the van der Waals, electrostatic and Lewis acid-base interactions described in the extended DVLO (XDVLO) theory (4). Despite the comprehensive nature of this model, discrepancies in the predictions when compared to experimentally derived data exposes a number of substantial flaws (5–7), particularly in the description of the interaction between biological moieties.

1 Atomic force microscopy (AFM) offer an answer to this issue allowing unique insights into the  
2 interaction processes of biological systems. Application of traditional AFM techniques allow for  
3 the unparalleled visualization and, characterization of the substrate topography at both the  
4 micro and nanometer scale. This has been applied to the characterization of bioprocess  
5 engineering surfaces such as stainless steel to measure surface roughness of different finishes  
6 pore size determination of separation membranes and study of cellular surfaces (8–10) AFM is  
7 not just an imaging device it also has a force measurement capability that has provided novel  
8 insight into the interactions of bioprocess engineering surfaces this includes the direct  
9 quantification of forces at the microbial surface and nano-mechanics allowing elucidation of the  
10 interplay of all of these factors under *in situ* conditions (11,12).

11

12 Through the course of this review the authors hopes to highlight the versatility of AFM.  
13 Summarize the landmark research that guided the application of the technology in the  
14 characterization of substrates, bacterial cells, and the adhesion forces and how these studies,  
15 build upon current microbial adhesion models that impact the characterization and optimization  
16 of bioprocess engineering surfaces.

17

## 18 **2 Basic Principles**

19 AFM is a form of high resolution microscopy from the family of scanning probe microscopies  
20 (SPM) developed in the mid-1980s the components of which are detailed in figure 1 (13). AFMs  
21 defining features are its resolution, demonstrated to be in the order of fractions of a nanometer,  
22 and versatility as a force sensor. AFM operates two major modes; imaging and force  
23 spectroscopy, the former can be further divided into two major categories of imaging; contact  
24 and intermittent-contact, the basic principles employed during operation remain the same  
25 regardless of application. Other AFM imaging techniques have been developed that map  
26 properties such as conductance and friction across a surface, however it is contact and  
27 intermittent contact mode that have mainly been applied to the study of process engineering  
28 surfaces.

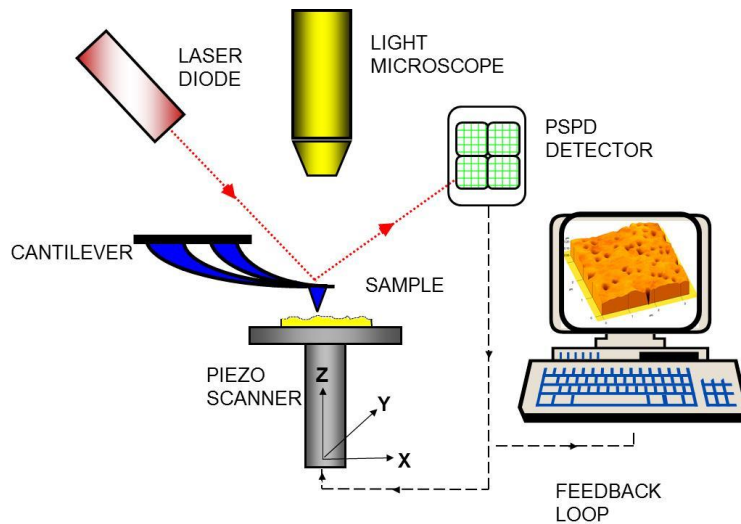


**Figure 1 Schematic representation of the atomic force microscope**

1  
2  
3  
4  
5 During measurement AFM records the nanoscale attractive and repulsive forces of the sample  
6 material by the deflection of a sharp tipped cantilever, which is systematically scanned across  
7 the surface. These forces are measured via the displacement of a laser reflected off the upper  
8 gold-coated side of the cantilever onto a quadratic photosensitive photodiode (PSPD). In  
9 contact mode, the AFM cantilever is brought into intimate contact with the sample material, the  
10 material is then rastered beneath the cantilever and axial and longitudinal deflections in the  
11 cantilever recorded via the photodiode. Intimate contact with the sample material is essential,  
12 and maintained through the implementation of a DC feedback amplifier controlling a  
13 piezoelectric motor to maintain a set level of deflection in the cantilever. This ensures that the  
14 force applied to the sample is constant and controlled to prevent sample damage. The forces in  
15 the bent cantilever maintain the imaging tip in direct contact with the surface. The destructive  
16 forces applied to the sample as a result of imaging can be mitigated through imaging in a liquid  
17 media and/or changing to intermittent-contact imaging. Additionally imaging in liquid allows for  
18 the removal of the strong attractive forces (capillary forces) on the AFM tip and cantilever  
19 caused by the adsorbed water layers at the surface of the sample further reducing the forces  
20 applied to the sample due to the tip. Imaging in a liquid media has the additional advantage of  
21 allowing for the characterization of sample materials such as membranes and biological  
22 contaminant under process- relevant conditions. However, due to the mobility of some bacterial  
23 species and the generally weak forces binding the cells to the surface, immobilization of the  
24 cells is often required to prevent destruction of the sample (14–16). Comprehensive review of  
25 the methods employed in the immobilization of bacterial cells can be found here (17). However,  
26 for the purposes of this review a brief summery shall be supplied. Typically immobilization takes  
27 one of two form; mechanical, or chemical. Mechanical immobilization traps the cells within an  
28 inert matrix for example, gelatin, agar or membranes (14,18–20). This methodology has been

1 refined to include the use of functionalized surfaces such as lithographically patterned silica and  
 2 polydimethylsiloxane (PDMS) (15,21–24). Chemical immobilization typically make use of  
 3 surface chemistry to bind the cell to substrate. The target for immobilization varies and includes  
 4 surface charge in the case of poly-L-lysine to the crosslinking of carboxyl groups (25–30). While  
 5 chemical techniques typically result in a high level of immobilization and specificity in orientation  
 6 care should be taken in selecting an appropriate technique. Chemical fixation, through its very  
 7 nature alters the surface chemistry of the cell and therefore alters not only the surface  
 8 properties but also the viability of the cell. Hence, it is critical that an appropriate methodology is  
 9 selected that takes into consideration the goals of the experimentation.

10 When imaging of soft samples such as biological samples or filtration membranes is required  
 11 application of contact mode imaging may not be suitable due to the intimate contact of the sharp  
 12 imaging tip with the surface, in this case intermittent contact or tapping mode is implemented.  
 13 During tapping mode, the cantilever is driven into oscillation at a frequency close to that of the  
 14 cantilevers resonance. The oscillation of the cantilever is then monitored as the sample material  
 15 is scanned with any alterations in the cantilevers oscillation corrected through the  
 16 implementation of a direct feedback loop, causing the movement of a piezo-scanner, which is  
 17 used to produce the image. The change in the oscillation as a function of the movement of the  
 18 piezo-scanner is then recorded as a topography image. Simultaneously, alteration in the phase  
 19 angle of the oscillations at the tip of the cantilever and the free oscillation of the cantilever can  
 20 be recorded. This allows for the characterization of the phase angle across the surface; termed  
 21 the phase contrast. Phase contrast mapping allows for a qualitative analyses of the differences  
 22 in the mechanical properties across a surface of heterogeneous material. Tapping mode offers  
 23 a number of advantages in the imaging of softer materials, most predominantly tapping mode  
 24 minimizes the destructive lateral forces of the technique on the sample material.  
 25

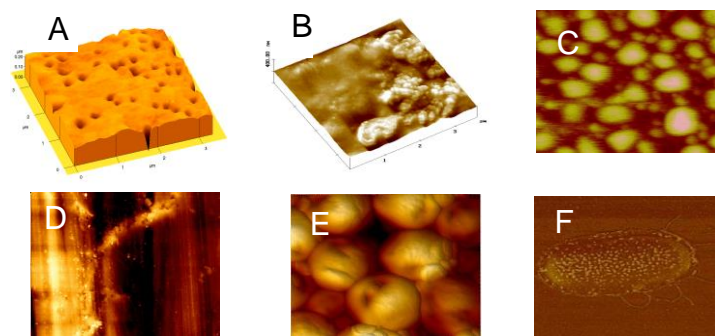


**Figure 2. AFM images of bioprocess engineering surfaces** (A) Cyclopore microfiltration membrane ( $3.2\mu\text{m}^2$ ) (B) Humic acid layer fouling an ultrafiltration membrane ( $3.5\mu\text{m}^2$ ) (C) Air bubbles at a membrane surface ( $0.75\mu\text{m}^2$ ) (D) Stainless steel process plant surface. ( $10\mu\text{m}^2$ ). (E) Lawn of *Saccharomyces cerevisiae* cells (brewing yeast NCYC 1681) showing budding scars ( $15\mu\text{m}^2$ ) (F) *Shewanella oneidensis* cell showing protein clusters at surface formed during anaerobic respiration and microbial fuel cell operation ( $1.2\mu\text{m}^2$ )

1 Figure 2 shows a number of example AFM images captured in our laboratory outlining the  
2 application of AFM in bioprocess engineering. The first three images are at membrane surfaces  
3 showing features important to process performance such as pore size and distribution (Figure 2  
4 (A)) Figure 2 (B) shows an ultrafiltration membrane purposely fouled with humic acids; a  
5 common foulant of process engineering surfaces consisting of the biproducts of organic matter  
6 biodegradation, Figure 2 (C) details bubbles at a membrane surface, which formed under  
7 certain operating conditions and are reported to participate in biofouling reduction (31). Finally  
8 figure 2 (D) details surface defect in a stainless steel surface as a result of surface polishing.  
9 These first four images highlight how AFM is capable of characterising a number of surface  
10 artifacts associated with fouling. Figure 2 also details AFM images that suggest molecular  
11 features of the microbial cell wall, in this particular case protein clusters involved in electron  
12 transport under anaerobic conditions (Figure 2 (E)); and yeast budding scars (Figure 2 (F)).  
13

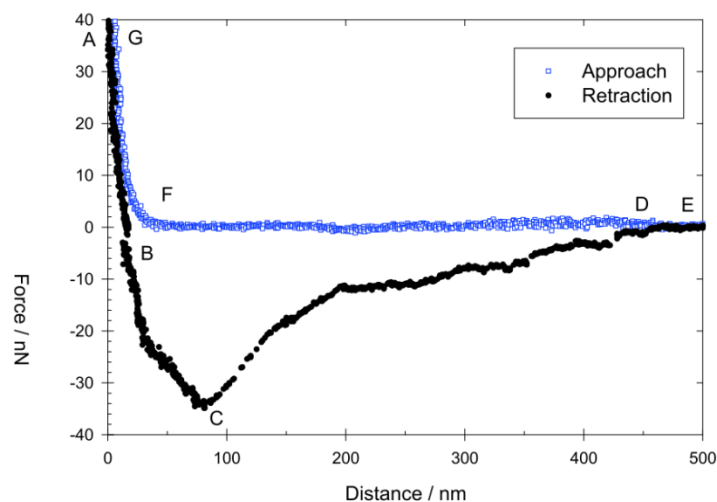


**Figure 3.** AFM Force spectroscopy of a single stationary phase *S. cerevisiae* cell probe against freshly cleaved mica in 0.01M NaCl pH5

14  
15  
16 Application of AFM is not limited to the characterization of topographical landscapes, in fact  
17 AFMs greatest asset lies in its ability to directly quantify the nanomechanical properties of a  
18 material. This is achieved through the generation of force-displacement curves; a graphical  
19 representation of the deflection of the cantilever as a function of the tip-sample separation  
20 distance as the tip is brought into contact with the sample. Figure 3 shows a typical force-  
21 displacement curve, in this case a single *S.cerevisiae* cell probe against(stationary phase)  
22 freshly cleaved mica. The force-displacement curve is treated as two curves; the approach



1 curve (E,D,F,G) and the retraction curve (A-D). At position E the sample and probe are in  
2 complete isolation this continues until position F wherein long range electrostatic forces begin to  
3 repel the probe. The probe is then pressed further towards the surface by the extension of the  
4 piezo scanner, through the electrostatic repulsion experienced at F until contact with the sample  
5 surface is achieved. At this point a number of nano-mechanical properties can be defined, such  
6 as elastic and plastic deformation regions and the yield point. The bending of the cantilever  
7 continues at the constant, defined approach speed until a predefined loading force is  
8 experienced (G). Point A defines the start of the retraction curve, the probe is retracted from the  
9 surface and any compression in the probe or surface is present to point B. Point C represents  
10 the separation of the probe from the sample material, in this case the probe exhibits some  
11 adhesion with the substrate as seen through the deflection of the cantilever in the opposite  
12 direction culminating in the snapping of the attractive forces at the apex wherein the cantilever  
13 returns to a state of zero deflection (E). This characteristic behavior allows for the generation of  
14 a number of key variables, for example, at point C the maximum adhesive force can be defined  
15 as the maximum deflection of the cantilever. Similarly, the energy of adhesion can also be  
16 defined as the area between the approach and retract curves. With regards to biological  
17 samples, this area is often large and not as “clean” as non-biological samples. This is for a  
18 variety of reasons, including multiple fracture points caused by the fracture of different  
19 macromolecules; discussed in depth later in this review, and the tendency for elastic  
20 deformation of biological samples. The nanomechanical properties of the substrate can be  
21 derived from the contact regions (F-G and A-B) and the adhesive properties from region B-D,  
22 however it is worth noting that these variables are dependent on the loading rate of the  
23 measurement.

24

25 Comparison of force-deflection curves collected from soft biological samples to those taken at  
26 samples with significantly higher mechanical properties such as silica can allow for the  
27 characterization of nanomechanical properties, such as Young’s modulus and turgor pressure.  
28 This is achieved by processing of the curves through a Hertzian model, which describes the  
29 elastic deformation of two homogenous bodies touching under load, assuming a parabolic  
30 indenter and that the cantilever is of significantly greater thickness than that of the indentation  
31 depth, the force can be defined by the equation;

32 
$$F(\delta)_{parabolic} = \frac{4E\sqrt{R}}{3(1-\nu^2)} \delta^{3/2}$$

33 where R is the radius of the indenter,  $\delta$  is the indentation depth, E the Young’s modulus and  $\nu$   
34 the poisson ratio. Assuming the prerequisites are met the definition of the indentation depth as a  
35 function of the applied force is then possible. However, in reality the first assumption; that the  
36 both bodies are homogenous, is often incorrect and in fact the substrate is heterogeneous in  
37 nature. Hence, multiple force curves at multiple surface locations this should be considered

1 when analyzing a homogenous substrate.. Furthermore, the act of nanoindentation is by its very  
2 definition a destructive process and as a result consecutive indentation of the same  
3 geographical location may result in variation.

4 It is worth noting that with the interpretation of force curves determination of the contact point is  
5 often necessary. This is particularly challenging for biological samples for several reasons.  
6 Firstly, there is the definition of contact, wherein contact of any description defines the zero  
7 point. This would be easily discernable if both objects were essentially smooth on the given  
8 scale of measurement; in this case the nanometer scale. However, this is far from the case and  
9 in fact both topographies, especially the biological one are likely to respectively rough due to the  
10 presence of surface macromolecules to name one obstruction. Methods for the calculation of  
11 the precise contact point have been developed, wherein scattered laser light shone between the  
12 colloid and the sample is detected using a near-field scanning optical microscope or inverted  
13 light microscope however they are far from simply employed. Secondly, on approaching the  
14 sample if the attractive forces exceed the spring constant of the cantilever then the cantilever  
15 will snap into contact with the sample, and then further drawn into the sample by the attractive  
16 forces. This results in two issues, firstly the contact point is almost impossible to define and  
17 secondly it is then necessary to assume that no indentation of the sample has occurred. While  
18 this is easily mitigated through selection of a cantilever with an appropriate spring constant it  
19 does limit resolution.

### 21 **3 Bacterial Adhesion and Biofouling**

#### 22 **3.1 Mechanisms and Theoretical Models**

23 Surface adhesion is a multistage event, consisting of initial or reversible adhesion followed by  
24 permanent or irreversible adhesion. Reversible adhesion defines the most crucial step in  
25 adsorption of the cell to the substrate, involving the simple, non-specific interaction of a number  
26 of fundamental physical effects including; van der Waals forces, Brownian motion, electrostatic,  
27 hydrophobic and acid-base interactions. While irreversible adhesion is more complex as it is the  
28 product of the characteristics of the cell, and predominately mediated by polymeric structures on  
29 the bacterial surface such as pili, flagella, adhesins and capsule components (slime layer,  
30 glycocalyx).

31  
32 Initially, attempts to model bacterial adhesion focused on the use simple colloidal models such  
33 as Derjaguin-Landau-Verwey-Overbeek (DLVO) (16,32,33). However experimental results have  
34 typically been shown to correlate poorly to predictions made by this method, as the DLVO  
35 theory only considers electrostatic and van der Waals forces (5). This may be a result of the  
36 inherent assumptions of DLVO theory, which suggests that pH and ionic strength are the  
37 defining features of bacterial adhesion in solution; while ignoring the effect of hydrophobicity,  
38 or, the incorrect estimation of key variables (6,7).The result of these discrepancies resulted in  
39 the combination of the DLVO theory and surface thermodynamics. While this remediated some

1 of the discrepancies of the DVLO theory a number of other phenomenon were still unaccounted  
 2 for, predominantly as a result of the assumptions of thermodynamic theory in which the reaction  
 3 is assumed to be reversible, and that a new intimate bacterium substrate interface is formed  
 4 (34–37). van Oss further extended the DVLO theory to include hydrophobic interactions (4).  
 5 Extended DVLO theory (XDVLO) as it became known, expressed the total adhesion energy of a  
 6 spherical object; the cell, against a semi-infinite plane; the substrate at a discrete distance to be  
 7 a result of the sum of the van der Waals, electrostatic and lewis acid-base interactions and is  
 8 defined by the equation:

$$\Delta G^{TOT}(d) = \Delta G^{LW}(d) + \Delta G^{EL}(d) + \Delta G^{AB}(d)$$

10 wherein  $\Delta G^{LW}(d)$ ,  $\Delta G^{EL}(d)$  and  $\Delta G^{AB}(d)$  are the free energies of the Lischitz-van der Waals,  
 11 electrostatic and Lewis acid-base interactions respectively at a given distance. At a discrete  
 12 distance  $d$ ,  $\Delta G^{LW}(d)$ ,  $\Delta G^{EL}(d)$  and  $\Delta G^{AB}(d)$  can be defined as:

$$\Delta G^{LW}(d) = -\frac{A}{6} \left[ \frac{a}{d} + \frac{a}{d+2a} + \ln \left( \frac{d}{d+2a} \right) \right]$$

$$\Delta G^{EL}(d) = \pi \epsilon a (\zeta_1^2 + \zeta_2^2) \left[ \frac{2\zeta_1\zeta_2}{\zeta_1^2 + \zeta_2^2} \ln \frac{1 + \exp(-\kappa d)}{1 - \exp(-\kappa d)} + \ln \{1 - \exp(-2\kappa d)\} \right]$$

$$\Delta G^{AB}(d) = 2\pi a \lambda \Delta G_{adh}^{AB} \exp \left[ \frac{(d_0 - d)}{\lambda} \right]$$

16 wherein  $a$  is the radius of the sphere,  $A$  is the Haymaker constant and defined as:

$$A = -12\pi d_0^2 \Delta G_{adh}^{LW}$$

18  $\zeta$  is the zeta potential,  $\epsilon$  is the permittivity of the medium  $K$  is the electric double layer thickness,  
 19  $\lambda$  is the correlation length if molecules in a liquid medium and  $d_0$  is the closest separation  
 20 distance between the sphere and plane. Finally,  $\Delta G_{adh}^{LW}$  and  $\Delta G_{adh}^{AB}$  are the free energies of  
 21 adhesion for the Lischitz-van der Waals, and Lewis acid-base interactions as defined by the  
 22 LW-AB approach. Through the implementation of this model a series of separation distance  
 23 against free energy graphs can be created theorizing the interactions between the cell and the  
 24 substrate. Through interpretation of these graphs maximum and minimum energy requirements  
 25 can be deduced for a given separation distance and hence favorability of the adhesion event.  
 26 However, while the theory proves to be a powerful tool in the modeling of the initial stages of  
 27 bacterial adhesion the model still fails to take into consideration the biological aspect of the  
 28 interaction such as the effects due to pilli, flagella and fails to account for non-spherical cell  
 29 shapes.. AFM offers a unique opportunity to remedy these issues. Firstly, through the  
 30 application of force spectroscopy; to be discussed in the section 4, AFM allows for the direct  
 31 quantification and comparison of experimentally derived approach curves and the theoretical  
 32 separation distance against free energy curves predicted by these models. Secondly, through  
 33 the characterization of the folding/unfolding pathways of surface macromolecules and the use of  
 34 non-spherical cell probes further refinement of the model through the implementation of a fourth  
 35 biological factor in the XDVLO theory may be possible. Consequently, the implementation of a

1 more rigorous theoretical framework will be possible for predicting and preventing biofouling at  
2 bioprocess engineering surfaces

### 4 **3.2 Substratum Characteristics**

#### 5 **3.2.1 Surface Roughness**

6 The effect of substratum characteristics on the adhesion of bacteria has been a point of interest  
7 ever since the discovery of the detrimental effects of biofilms, with both surface roughness and  
8 nanomechanical properties being implicated with increasing retention of bacteria [31]. However,  
9 due to its complex nature elucidating the complete mechanism of bacterial attachment and  
10 biofouling of bioprocess surfaces remains a challenge. As shown by the XDVLO theory the  
11 physiochemical interactions are understood to a degree although not comprehensively; the  
12 impact of surface topography on the adhesive characteristics remains less well defined. To  
13 begin to elucidate the mechanism by which bacterial adhesion is influenced by surface  
14 roughness a method for quantifying surface roughness is required. A number of techniques are  
15 available to researchers to accomplish this such as stylus and optical type profilometers and  
16 dynamic contact angle. These techniques offer a number of advances such as being relatively  
17 simple to implement and not particularly resource intensive, but their resolution is limited to the  
18 microscale and offer no further insight into the substrate characteristics. As a result, more  
19 researchers are applying AFM to the characterization of such surfaces. AFM offers a number of  
20 key features not achievable through other means, most notably its ability to resolve the surface  
21 roughness at the nanometer scale: a scale that has grown in interest over the last few years  
22 (38,39).

23 Several studies have been completed detailing the effect of surface roughness on bacterial  
24 adhesion (10-18). The consensus of the aforementioned studies being that on the micro-scale,  
25 bacterial adhesion is at its peak when the [arithmetic](#) roughness ( $R_a$ ) of the surface nears the  
26 diameter of the cell. This correlation between surface adhesion and surface roughness has  
27 been attributed to a number of factors, including the maximization of surface contact area, the  
28 accumulation of organic contaminants and protection from sheer stresses (40–42).  
29 Consequently, modification of substrate  $R_a$  has become a primary focus in the formation of  
30 antifouling strategies.

31 Interest in minimizing the surface roughness of substrate materials has resulted in a growth in  
32 the characterization and application of nanoscale topographies (43–47). However, nanoscale  
33 interactions have proved to be more complex with a number of fundamental contradictions  
34 arising (48–54). For example, a significant increase in the adhesion of *Escherichia coli* and  
35 *Pseudomonas aeruginosa* on nanorough thin film titanium substrates was observed in  
36 comparison to a flat reference samples(46). The authors attribute this to the physical stimulus of  
37 the nanotextured surface. However, the authors proceed to describe the absence of flagella on  
38 *P. aeruginosa* cells bound to same surface, suggesting changes in cell surface characteristics.  
39 Conversely, in direct opposition to the previously mentioned study Ivanova *et al.* reported that

1 on comparable titanium surfaces adhesion of *P. aeruginosa* and *S. aureus* were inversely  
2 proportional to the roughness of the surface (43,47). However it is worth noting that a number of  
3 the studies performed on titanium contain quantities of TiO<sub>2</sub>, a known antibacterial. It is  
4 therefore difficult to distinguish alterations in adhesion caused by the nanoscale roughness of  
5 the surface as opposed to those caused by the antimicrobial activity.

6 In a more recent study the effect of nanotopography and grain size, on the adhesion of *E. coli*,  
7 *P. aeruginosa*, *S. epidermidis* and *S. aureus* was observed on shot peened SS316L stainless  
8 steel (55). During the study the authors suggest that increases in the nanoscale roughness of  
9 material notably increased the adhesion rate of both *S. aureus* and *S. epidermidis* while having  
10 no significant effect on the adhesion rate of the two Gram negative species. The research group  
11 were additionally able to conclude that the refinement of the grain size, as a result of shot  
12 peening did not significantly alter adhesion rates.

### 13 14 **3.2.3 Conditioning Layers**

15 Adsorption of organic matter to surfaces in aqueous environments and the corresponding  
16 impact on bacterial adhesion rates has been well documented (56–62). A major contributing  
17 factor to the formation of an organic conditioning layer is the deposition of extracellular  
18 polymeric substance (EPS). EPS is not a defined mixture but rather the collective name given to  
19 a number of soluble macromolecules produced by bacteria. EPS has been demonstrated to  
20 consist of a temporally dynamic mix of polysaccharides, DNA, lipids, proteins and humic  
21 substances (63–66). EPS can be loosely grouped into two forms when viewed with regards to  
22 planktonic cells, loosely bound (LB-EPS) and tightly bound (TB-EPS), both varying in  
23 composition and the former being the primary form of EPS conditioning layers and composed  
24 primarily of bacterial proteins and the latter bacterial capsids (67,68). While the formation of  
25 organic conditioning layers effects all surfaces within a process engineering environment, by far  
26 the most researched area is in the organic fouling of membranes (69–71).

27 Application of membrane separation technologies has become a substantial part of a number of  
28 industrial processes including membrane bioreactors, desalination plants and food processing.  
29 However, with all sizes of membrane; microfiltration, ultrafiltration, nanofiltration and reverse  
30 osmosis (RO), biofouling is of particular concern as colonization of the membrane will typically  
31 result in reductions in membrane separation efficiency and eventually biodeterioration of the  
32 separation membrane surface and surrounding infrastructure (72).

33 In a recent study, Suwarno *et al.*, characterized the effects of a number of conditioning layer  
34 contaminants on bacterial adhesion of RO membranes (73). During the study, the researchers  
35 observed no trend in organic fouling and surface roughness with an increase in surface  
36 roughness of 19nm when the membrane was fouled with alginic acid, this was compared to a  
37 21nm and 15nm decrease in surface roughness for a bovine serum albumin fouled membrane  
38 and membrane bioreactor permeate fouled membrane, respectively. Suwarno *et al.*, continued  
39 to use AFM to characterize the adhesive properties of the membranes, during the force

1 measurement study it was found that the adhesive force exhibited at the membrane surface  
2 was significantly increased from the baseline when exposed to the model foulants; alginic acid  
3 and bovine serum albumin [55]. However, the change in adhesion was less pronounced with  
4 contamination of membrane bioreactor permeate; an increase of 110nN was observed. The  
5 group attributed this to be a result of non-uniform distribution of the foulant material. The  
6 research identified an increase in bacterial adhesion as a result of the biopolymer fouling.  
7 Bacterial adhesion to the membrane bioreactor permeate fouled membranes was found to be in  
8 the order of four times higher than that of the virgin membranes indicating that these changes in  
9 surface roughness and adhesion correlate to an increase in bacterial retention.

### 10 **3.3 Force Spectroscopy**

11 Implementation of AFM for the characterization of bacterial nano-mechanics has been widely  
12 accepted as an essential tool in the microbiological community. Eager adoption of AFM by the  
13 community is the result of the ability of AFM to resolve the nano-mechanical properties of cells  
14 on all levels, from single molecules to consortia of multiple cells such as biofilms in the nano  
15 and picoNewton range (74). Understanding the nano-mechanics of bacterial cells with regards  
16 to the cellular capsid, elastic modulus and turgor pressure is of particular importance in the  
17 further refinement of the understanding of reversible attachment. While, characterization of  
18 membrane bound polyproteins, adhesins and cellular organelles will further understanding of  
19 the mechanisms of irreversible attachment.

#### 21 **3.3.1 Single Molecule Force Spectroscopy (SMFS)**

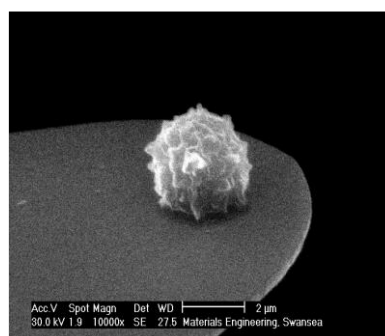
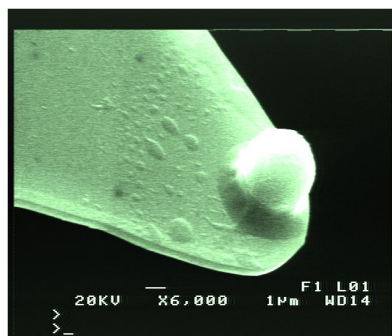
22 Surface macromolecules are essential for the ubiquitous success of microbes within the  
23 environment, mediating a number of physiological processes including adhesion. Chemical  
24 functionalization of the cantilever has allowed AFM to be applied in the characterisation of a  
25 number of surface bound receptors important in adhesion under *in situ* conditions including  
26 lipopolysaccharides, pilli and adhesins (75–82). The study of surface macromolecules has  
27 facilitated the rapid development of SMFS techniques, and ensured a comprehensive  
28 understanding of the fundamental mechanics governing tip-molecules interactions (83–85).

29 Microbial surface proteins can be generally broken down into two groups: functional surface  
30 proteins such as adhesins and surface bound long chain macromolecules such as pili. AFM  
31 characterisation of long chain surface macromolecules is complex. However, through the use of  
32 established models such as the Worm Like Chain (WLC) and Freely Jointed Chain (FJC)  
33 models a wealth of information on adhesion can be ascertained. Use of the WLC and FJC  
34 models allow for the definition of the entropic elasticity of the molecules and as the result the  
35 contour length ( $L_o$ ) (86,87). If the structure of the target macromolecule is unknown, definition of  
36  $L_o$  allows for the confirmation of the experimentally derived data through the use of a normal  
37 (Gaussian) distribution, while simultaneously partially elucidating the unbinding pathway  
38 (88,89). This method for the definition of  $L_o$  was further expanded through the work of Farrance  
39 *et al.*, wherein an idealized theoretical tethered surfaces and the probability of two such

1 surfaces contacting is used to predict the distribution of experimentally derived data (90). In a  
2 recent example, SMFS was applied to demonstrate the role of *P. aeruginosa* type IV pili (91).  
3 During the study the group utilised a *pilT* mutant to demonstrate low-affinity, high-avidity model  
4 for type IV pili adhesion through the application of the WLC model. The group concluded that  
5 each subunit of PilA contained an adhesin site capable of binding the surface allowing adhesion  
6 along the full length of the molecule.

### 8 3.3.2 Single Cell Force Spectroscopy

9 Pioneered through the construction of a *S. cerevisiae* cell probes by Bowen *et al.*, single-cell  
10 force spectroscopy (SCFM) has become a fundamental technique in adhesive force  
11 characterization (92). This technique is of particular importance in the field of bacterial adhesion  
12 as it allows for the simultaneous quantification of all factors governing adhesion under *in situ*  
13 conditions, therefore reducing error as the result of the interpretation of discrete elements.  
14 Selection of an appropriate immobilization technique is imperative in the construction of an AFM  
15 cell probe (Figure 4). As a result a number of techniques have been utilized to functionalize  
16 cantilevers including chemical fixation, electrostatic and wet adhesives (93–100). With the  
17 optimum method allowing for the immobilization of the target cell with minimal effect of the  
18 technique on the viability, and physiochemical properties of the immobilized cell. Further  
19 consideration needs to be taken in to the size of the target cell, with larger cells; such as *S*  
20 *cerivisae* (~10 $\mu$ m) being easily immobilized directly to the cantilever surface. While  
21 immobilization of smaller cells and spores; such as bacteria (~1 $\mu$ m) require further steps. In one  
22 such method to immobilize a single bacterial cell, a colloidal sphere was immobilized onto the  
23 tip of an AFM cantilever. This colloid was then further functionalized with polydopamine to facilitate  
24 the immobilization of a single bacterium through AFM micromanipulation (101). This technique  
25 offered a number of significant advantages over comparable techniques for the immobilization  
26 of single cells. Firstly, through the use of confocal microscopy the technique was shown to  
27 immobilize bacterial cells with minimal effect on the target cells membrane integrity, and as a  
28 result the viability of that cell. Additionally, the technique allows for the immobilization of the  
29 target cell in a highly organized manner further increasing the repeatability of the  
30 measurements. Finally the technique was found to be applicable to a number of target species  
31 (99).



1  
2 **Figure 4.** SEM image of a cell probe A) *Saccharomyces cerevisiae* B)  
3 *Aspergillus niger*  
4  
5

6 In a recent study, SCFS was applied to characterize the effect of antifouling polymer brushes on  
7 the adhesion of *Yersinia pseudotuberculosis* (102). During the study the group compared the  
8 adhesive forces, energy of adhesions and the rupture distance of the brushes against  
9 polytetrafluoroethylene (PTFE), polystyrene and glass controls. It was found that the adhesive  
10 forces exhibited by the bacteria were sustainably reduced, with a 22% reduction observed for  
11 the oligo(ethyleneglycol) methyl ether methacrylate (MeOEGMA) and oligo(ethyleneglycol)  
12 methacrylate (HOEGMA) brushes and no less than a 95% reduction for the *N*-(2-hydroxypropyl)  
13 methacrylamide (poly(HPMA)), (3-acryloylamino-propyl)- (2-carboxyethyl)-dimethyl-ammonium  
14 (CBAA), [2-(methacryloyloxy)ethyl]- dimethyl-(3-sulfopropyl)ammonium hydroxide (SBMA), 2-  
15 methacryloyloxyethyl phosphorylcholine (PCMA), and, Poly(2-hydroxyethyl methacrylate) (poly-  
16 (HEMA)) brushes. Similarly the energy of adhesion showed a significant decrease from 450,  
17 550 and 7000aJ for the glass, PTFE and PS respectively to 100aJ for the oligo(ethylene glycol)  
18 methactylates and 10aJ for the polyzwitterioic and poly(HPMA) brushes. Further analyses of the  
19 force-distance curves highlighted a decrease in the number of rupture events with a  
20 corresponding increase in the event distance. A further comprehensive study conducted by  
21 Aguayo *et al.*, investigated the impact of nanopatterned polycarbonate on *S. aureus* adhesion  
22 (103). During the study the group observed an increase in both the adhesive force and energy  
23 of adhesion with increasing contact time and nanopatterning. Interestingly, the number and  
24 location of rupture events exhibited remained relatively constant, the researchers suggested  
25 that the surface and/or capsular receptors were involved in adhesion to both substrates  
26

#### 27 **4 Conclusions**

28 In conclusion, AFM has become an essential tool for the study of bioprocess engineering  
29 surfaces. This is exemplified by the comprehensive insight it has provided into the nanoscale  
30 forces involved in bacterial adhesion and their mechanical properties. Through the  
31 characterization of nanoscale surface topography AFM has allowed for the elucidation of the  
32 effect of surface roughness on bacterial adhesion rates adding further experimental evidence to  
33 the predictions of adhesion models and in turn informing potential anti-fouling strategies.  
34 Studies into microbial conditioning have demonstrated the heterogeneity of the conditioning  
35 layer while demonstrating the importance of this layer in bacterial adhesion and alluding to  
36 potential methods to prevent, remove or mitigate the effect. Conversely AFM has been used to  
37 demonstrate the efficacy of anti-fouling layers. Through the functionalisation of probes attached  
38 to AFM cantilevers, SMFS has revolutionised our understanding of the complex interplay  
39 between microbial surface macromolecules under *in situ* conditions providing valuable insight



1 into new strategies of preventing the initiation of irreversible attachment. SCFM has now  
2 become a mainstay in microbial applications of AFM, and the study of microbial colonisation of  
3 bioprocess engineering surfaces. SCFM studies has demonstrated the efficacy of a number of  
4 antifouling strategies while facilitating whole cell studies to further future modelling. AFM is not  
5 without its limitations and most applications of the technology still require the immobilisation of  
6 the cells prior to measurement, potentially influencing the validity of the measurement. Despite  
7 this AFM is still an essential addition to the family of instruments used in the characterization of  
8 bioprocess engineering surfaces and bacteria. The technology promises further analytical  
9 capabilities for the study of microbial systems with the only limitation being the imagination  
10 needed to invent more ingenious functionalised cantilever probes.

11

12

13 **Conflict of interest**

14 The authors declare no financial or commercial conflict of interest.

15

16

## 1 5 References

- 2 1. Valle J, Burgui S, Langheinrich D, Gil C, Solano C, Toledo-Arana A, et al. Evaluation of  
3 Surface Microtopography Engineered by Direct Laser Interference for Bacterial Anti-  
4 Biofouling. *Macromol Biosci* [Internet]. 2015 Aug;15(8):1060–9. Available from:  
5 <http://doi.wiley.com/10.1002/mabi.201500107>
- 6 2. Chan WF, Marand E, Martin SM. Novel zwitterion functionalized carbon nanotube  
7 nanocomposite membranes for improved RO performance and surface anti-biofouling  
8 resistance. *J Memb Sci*. 2016;509:125–37.
- 9 3. Pechook S, Sudakov K, Polishchuk I, Ostrova I, Zakin V, Pokroy B, et al. Bioinspired  
10 Passive Anti-biofouling Surfaces Preventing Biofilm Formation. *J Mater Chem B*.  
11 2014;4(8):1166–9.
- 12 4. Van Oss CJ. Energetics of Cell-Cell and Cell -Biopolymer Interactions. *Cell Biophys*.  
13 1989;14:1–16.
- 14 5. Poortinga AT, Bos R, Norde W, Busscher HJ. Electric double layer interactions in  
15 bacterial adhesion to surfaces. *Surface Science Reports*. 2002. 1-32 p.
- 16 6. Dan N. The effect of charge regulation on cell adhesion to substrates: Salt-induced  
17 repulsion. *Colloids Surfaces B Biointerfaces*. 2003;27(1):41–7.
- 18 7. Duval JFL, Busscher HJ, Van De Belt-Gritter B, van der Mei HC, Norde W. Analysis of  
19 the Interfacial Properties of Fibrillated and Nonfibrillated Oral Streptococcal Strains from  
20 Electrophoretic Mobility and Titration Measurements: Evidence for the Shortcomings of  
21 the “Classical Soft-Particle Approach.” *Langmuir* [Internet]. 2005 Nov;21(24):11268–82.  
22 Available from: <http://pubs.acs.org/doi/abs/10.1021/la051735q>
- 23 8. Bowen WR, Lovitt RW, Wright CJ. Atomic force microscope studies of stainless steel :  
24 Surface morphology and colloidal particle adhesion. 2001;6:623–9.
- 25 9. Francis LW, Lewis PD, Gonzalez D, Ryder T a, Webb G, Joels L a, et al. Progesterone  
26 induces nano-scale molecular modifications on endometrial epithelial cell surfaces. *Biol*  
27 *Cell* [Internet]. 2009;101(8):481–93. Available from:  
28 <http://www.ncbi.nlm.nih.gov/pubmed/19236310>
- 29 10. Johnson D, Hilal N. Characterisation and quantification of membrane surface properties

- 1 using atomic force microscopy: A comprehensive review. *Desalination*. 2015. p. 149–64.
- 2 11. Powell LC, Pritchard MF, Emanuel C, Onsøyen E, Rye PD, Wright CJ, et al. A  
3 nanoscale characterization of the interaction of a novel alginate oligomer with the cell  
4 surface and motility of *Pseudomonas aeruginosa*. *Am J Respir Cell Mol Biol*.  
5 2014;50(3):483–92.
- 6 12. Bowen WR, Lovitt RW, Wright CJ. Atomic Force Microscopy Study of the Adhesion of  
7 *Saccharomyces cerevisiae*. *J Colloid Interface Sci* [Internet]. 2001;237(1):54–61.  
8 Available from: <http://www.ncbi.nlm.nih.gov/pubmed/11334514>
- 9 13. Binnig G, Quate C, Gerber C. Atomic Force Microscope [Internet]. *Physical Review*  
10 *Letters*. 1986. p. 930–3. Available from:  
11 <http://link.aps.org/doi/10.1103/PhysRevLett.56.930>  
12 6513-EAC6-4BC0-A144-AB381B706D40
- 13 14. Touhami A, Jericho MH, Beveridge TJ. Atomic force microscopy of cell growth and  
14 division in *Staphylococcus aureus*. *J Bacteriol*. 2004;186(11):3286–95.
- 15 15. Kailas L, Ratcliffe EC, Hayhurst EJ, Walker MG, Foster SJ, Hobbs JK. Immobilizing live  
16 bacteria for AFM imaging of cellular processes. *Ultramicroscopy*. 2009;109(7):775–80.
- 17 16. Marshall KC, Stout R, Mitchell R. Mechanism of the Initial Events in the Sorption of  
18 Marine Bacteria to Surfaces. *Journal of General Microbiology*. 1971. p. 337–48.
- 19 17. James SA, Powell LC, Wright CJ. Atomic Force Microscopy of Biofilms- Imaging,  
20 Interactions, and Mechanics. In: Dhanasekaran D, editor. *Microbial Biofilms - Importance*  
21 *and Applications*. InTech; 2016.
- 22 18. Gad M, Ikai A. Method for immobilizing microbial cells on gel surface for dynamic AFM  
23 studies. *Biophys J*. 1995;69(6):2226–33.
- 24 19. Kasas S, Ikai A. A method for anchoring round shaped cells for atomic force microscope  
25 imaging. *Biophys J*. 1995;68(5):1678–80.
- 26 20. Ahimou F, Touhami A, Dufrêne YF. Real-time imaging of the surface topography of living  
27 yeast cells by atomic force microscopy. *Yeast*. 2003;20(1):25–30.
- 28 21. Yao X, Walter J, Burke S, Stewart S, Jericho MH, Pink D, et al. Atomic force microscopy  
29 and theoretical considerations of surface properties and turgor pressures of bacteria.

- 1 Colloids Surfaces B Biointerfaces. 2002;23(2–3):213–30.
- 2 22. Vadillo-Rodríguez V, Busscher HJ, Norde W, De Vries J, Dijkstra RJB, Stokroos I, et al.  
3 Comparison of atomic force microscopy interaction forces between bacteria and silicon  
4 nitride substrata for three commonly used immobilization methods. *Appl Environ*  
5 *Microbiol.* 2004;70(9):5441–6.
- 6 23. Cerf A, Cau JC, Vieu C, Dague E. Nanomechanical properties of dead or alive single-  
7 patterned bacteria. *Langmuir.* 2009;25(10):5731–6.
- 8 24. Formosa C, Pillet F, Schiavone M, Duval RE, Ressler L, Dague E. Generation of living  
9 cell arrays for atomic force microscopy studies. *Nat Protoc [Internet].* 2014 Dec  
10 31;10(1):199–204. Available from:  
11 <http://www.nature.com/doi/10.1038/nprot.2015.004>
- 12 25. Bolshakova A V., Kiselyova OI, Filonov AS, Frolova OY, Lyubchenko YL, Yaminsky I V.  
13 Comparative studies of bacteria with an atomic force microscopy operating in different  
14 modes. In: *Ultramicroscopy.* 2001. p. 121–8.
- 15 26. Micic M, Hu D, Suh YD, Newton G, Romine M, Lu HP. Correlated atomic force  
16 microscopy and fluorescence lifetime imaging of live bacterial cells. *Colloids Surfaces B*  
17 *Biointerfaces.* 2004;34(4):205–12.
- 18 27. Arnoldi M, Fritz M, Bäuerlein E, Radmacher M, Sackmann E, Boulbitch A. Bacterial  
19 turgor pressure can be measured by atomic force microscopy. *Phys Rev E - Stat*  
20 *Physics, Plasmas, Fluids, Relat Interdiscip Top.* 2000;62(1 B):1034–44.
- 21 28. Parikh SJ, Chorover J. ATR-FTIR spectroscopy reveals bond formation during bacterial  
22 adhesion to iron oxide. *Langmuir.* 2006;22(20):8492–500.
- 23 29. Doktycz MJ, Sullivan CJ, Hoyt PR, Pelletier DA, Wu S, Allison DP. AFM imaging of  
24 bacteria in liquid media immobilized on gelatin coated mica surfaces. *Ultramicroscopy.*  
25 2003;97(1–4):209–16.
- 26 30. Camesano TA, Liu Y, Datta M. Measuring bacterial adhesion at environmental interfaces  
27 with single-cell and single-molecule techniques. *Adv Water Resour.* 2007;30(6–7):1470–  
28 91.
- 29 31. Johnson DJ, Al Malek SA, Al-Rashdi BAM, Hilal N. Atomic force microscopy of

- 1 nanofiltration membranes: Effect of imaging mode and environment. *J Memb Sci.*  
2 2012;389:486–98.
- 3 32. Verwey EJW. Theory of the stability of lyophobic colloids. *The Journal of physical and*  
4 *colloid chemistry.* 1947. p. 631–6.
- 5 33. Derjaguin B, Landau L. Theory of the stability of strongly charged lyophobic sols and of  
6 the adhesion of strongly charged particles in solutions of electrolytes. *Prog Surf Sci.*  
7 1993;43(1–4):30–59.
- 8 34. Fletcher M, Pringle JH. The effect of surface free energy and medium surface tension on  
9 bacterial attachment to solid surfaces. *J Colloid Interface Sci.* 1985;104(1):5–14.
- 10 35. Pratt-Terpstra IH, Weerkamp a H, Busscher HJ. Adhesion of oral streptococci from a  
11 flowing suspension to uncoated and albumin-coated surfaces. *J Gen Microbiol [Internet].*  
12 1987;133(11):3199–206. Available from: <http://www.ncbi.nlm.nih.gov/pubmed/3446750>
- 13 36. Rutter PR, Vincent B. Physicochemical Interactions of the Substratum, Microorganisms,  
14 and the Fluid Phase. In: Marshall KC, editor. *Microbial Adhesion and Aggregation:*  
15 *Report of the Dahlem Workshop on Microbial Adhesion and Aggregation Berlin 1984,*  
16 *January 15--20 [Internet]. Berlin, Heidelberg: Springer Berlin Heidelberg; 1984. p. 21–38.*  
17 Available from: [http://dx.doi.org/10.1007/978-3-642-70137-5\\_3](http://dx.doi.org/10.1007/978-3-642-70137-5_3)
- 18 37. Pratt-Terpstra IH, Weerkamp AH, Busscher HJ. On a relation between interfacial free  
19 energy-dependent and noninterfacial free energy-dependent adherence of oral  
20 streptococci to solid substrata. *Curr Microbiol [Internet].* 1988 Nov;16(6):311–3.  
21 Available from: <http://link.springer.com/10.1007/BF01568537>
- 22 38. Truong VK, Lapovok R, Estrin YS, Rundell S, Wang JY, Fluke CJ, et al. The influence of  
23 nano-scale surface roughness on bacterial adhesion to ultrafine-grained titanium.  
24 *Biomaterials.* 2010;31(13):3674–83.
- 25 39. Arnold JW, Bailey GW. Surface finishes on stainless steel reduce bacterial attachment  
26 and early biofilm formation: scanning electron and atomic force microscopy study. *Poult*  
27 *Sci.* 2000;79(12):1839–45.
- 28 40. Boyd RD, Verran J, Jones M V., Bhakoo M. Use of the atomic force microscope to  
29 determine the effect of substratum surface topography on bacterial adhesion. *Langmuir.*

- 1 2002;18(6):2343–6.
- 2 41. Whitehead KA, Colligon J, Verran J. Retention of microbial cells in substratum surface  
3 features of micrometer and sub-micrometer dimensions. *Colloids Surfaces B*  
4 *Biointerfaces*. 2005;41(2–3):129–38.
- 5 42. Bohinc K, Dražić G, Abram A, Jevšnik M, Jeršek B, Nipič D, et al. Metal surface  
6 characteristics dictate bacterial adhesion capacity. *Int J Adhes Adhes*. 2016;68:39–46.
- 7 43. Ivanova EP, Truong VK, Wang JY, Berndt CC, Jones RT, Yusuf II, et al. Impact of  
8 nanoscale roughness of titanium thin film surfaces on bacterial Retention. *Langmuir*.  
9 2010;26(3):1973–82.
- 10 44. Lüdecke C, Bossert J, Roth M, Jandt KD. Physical vapor deposited titanium thin films for  
11 biomedical applications: Reproducibility of nanoscale surface roughness and microbial  
12 adhesion properties. *Appl Surf Sci*. 2013;280:578–89.
- 13 45. Truong VK, Rundell S, Lapovok R, Estrin Y, Wang JY, Berndt CC, et al. Effect of  
14 ultrafine-grained titanium surfaces on adhesion of bacteria. *Appl Microbiol Biotechnol*.  
15 2009;83(5):925–37.
- 16 46. Singh AV, Galluzzi M, Borghi F, Indrieri M, Vyas V, Podestà A, et al. Interaction of  
17 bacterial cells with cluster-assembled nanostructured titania surfaces: an atomic force  
18 microscopy study. *J Nanosci Nanotechnol [Internet]*. 2013;13(1):77–85. Available from:  
19 <http://www.ncbi.nlm.nih.gov/pubmed/23646700>
- 20 47. Ivanova EP, Truong VK, Webb HK, Baulin VA, Wang JY, Mohammadi N, et al.  
21 Differential attraction and repulsion of *Staphylococcus aureus* and *Pseudomonas*  
22 *aeruginosa* on molecularly smooth titanium films. *Sci Rep [Internet]*. 2011;1:165.  
23 Available from:  
24 [http://www.pubmedcentral.nih.gov/articlerender.fcgi?artid=3240996&tool=pmcentrez&re](http://www.pubmedcentral.nih.gov/articlerender.fcgi?artid=3240996&tool=pmcentrez&rendertype=abstract)  
25 [ndertype=abstract](http://www.pubmedcentral.nih.gov/articlerender.fcgi?artid=3240996&tool=pmcentrez&rendertype=abstract)
- 26 48. Singh AV, Vyas V, Patil R, Sharma V, Scopelliti PE, Bongiorno G, et al. Quantitative  
27 Characterization of the Influence of the Nanoscale Morphology of Nanostructured  
28 Surfaces on Bacterial Adhesion and Biofilm Formation. Bansal V, editor. *PLoS One*  
29 [Internet]. 2011 Sep 26;6(9):e25029. Available from:

- 1 <http://dx.plos.org/10.1371/journal.pone.0025029>
- 2 49. Mitik-Dineva N, Wang J, Stoddart PR, Crawford RJ, Ivanova EP. Nano-structured  
3 surfaces control bacterial attachment. In: Proceedings of the 2008 International  
4 Conference on Nanoscience and Nanotechnology, ICONN 2008. 2008. p. 113–6.
- 5 50. Park MR, Banks MK, Applegate B, Webster TJ. Influence of nanophase titania  
6 topography on bacterial attachment and metabolism. *Int J Nanomedicine*.  
7 2008;3(4):497–504.
- 8 51. Mitik-Dineva N, Wang J, Truong VK, Stoddart PR, Malherbe F, Crawford RJ, et al.  
9 Differences in colonisation of five marine bacteria on two types of glass surfaces.  
10 Biofouling [Internet]. 2009 Jul 3;25(7):621–31. Available from:  
11 <http://www.tandfonline.com/doi/abs/10.1080/08927010903012773>
- 12 52. Díaz C, Schilardi PL, Dos Santos Claro PC, Salvarezza RC, Fernández Lorenzo De  
13 Mele MA. Submicron trenches reduce the *Pseudomonas fluorescens* colonization rate  
14 on solid surfaces. *ACS Appl Mater Interfaces*. 2009;1(1):136–43.
- 15 53. Schaer-Zammaretti P, Ubbink J. Imaging of lactic acid bacteria with AFM - Elasticity and  
16 adhesion maps and their relationship to biological and structural data. *Ultramicroscopy*.  
17 2003;97(1–4):199–209.
- 18 54. Puckett SD, Taylor E, Raimondo T, Webster TJ. The relationship between the  
19 nanostructure of titanium surfaces and bacterial attachment. *Biomaterials*.  
20 2010;31(4):706–13.
- 21 55. Bagherifard S, Hickey DJ, de Luca AC, Malheiro VN, Markaki AE, Guagliano M, et al.  
22 The influence of nanostructured features on bacterial adhesion and bone cell functions  
23 on severely shot peened 316L stainless steel. *Biomaterials*. 2015;73:185–97.
- 24 56. Neihof R, Loeb G. DISSOLVED ORGANIC MATTER IN SEAWATER AND THE  
25 ELECTRIC CHARGE OF IMMERSSED SURFACES. *J Mar Res*. 1974;32(1):5–12.
- 26 57. Schneider RP, Leis A. Conditioning Films in Aquatic Environments. In: *Encyclopedia of*  
27 *Environmental Microbiology* [Internet]. Hoboken, NJ, USA: John Wiley & Sons, Inc.;  
28 2003. Available from: <http://doi.wiley.com/10.1002/0471263397.env036>
- 29 58. Dufrene YF, Vermeiren H, Vanderleyden J, Rouxhet PG. Direct evidence for the

- 1 involvement of extracellular proteins in the adhesion of *Azospirillum brasilense*.  
2 Microbiol. 1996;142:855–865.
- 3 59. Gómez-Suárez C, Pasma J, van der Borden AJ, Wingender J, Flemming HC, Busscher  
4 HJ, et al. Influence of extracellular polymeric substances on deposition and redeposition  
5 of *Pseudomonas aeruginosa* to surfaces. Microbiology. 2002;148(4):1161–9.
- 6 60. Hwang G, Liang J, Kang S, Tong M, Liu Y. The role of conditioning film formation in  
7 *Pseudomonas aeruginosa* PAO1 adhesion to inert surfaces in aquatic environments.  
8 Biochem Eng J [Internet]. Elsevier B.V.; 2013;76:90–8. Available from:  
9 <http://dx.doi.org/10.1016/j.bej.2013.03.024>
- 10 61. Hwang G, Kang S, El-Din MG, Liu Y. Impact of conditioning films on the initial adhesion  
11 of *Burkholderia cepacia*. Colloids Surfaces B Biointerfaces. 2012;91(1):181–8.
- 12 62. Hwang G, Kang S, El-Din MG, Liu Y. Impact of an extracellular polymeric substance  
13 (EPS) precoating on the initial adhesion of *Burkholderia cepacia* and *Pseudomonas*  
14 *aeruginosa*. Biofouling [Internet]. 2012;28(6):525–38. Available from:  
15 <http://www.ncbi.nlm.nih.gov/pubmed/22686692>
- 16 63. Wingender J, Strathmann M, Rode A, Leis A, Flemming H-C. Isolation and biochemical  
17 characterization of extracellular polymeric substances from *Pseudomonas aeruginosa*.  
18 In: Methods in Enzymology [Internet]. 2001. p. 302–14. Available from:  
19 <http://www.sciencedirect.com/science/article/pii/S0076687901365977>
- 20 64. Conrad A, Kontro M, Keinänen MM, Cadoret A, Faure P, Mansuy-Huault L, et al. Fatty  
21 acids of lipid fractions in extracellular polymeric substances of activated sludge flocs.  
22 Lipids [Internet]. 2003;38(10):1093–105. Available from:  
23 <http://link.springer.com/10.1007/s11745-006-1165-y>
- 24 65. Flemming H-C, Wingender J. Extracellular Polymeric Substances (EPS): Structural,  
25 Ecological and Technical Aspects. In: Encyclopedia of Environmental Microbiology  
26 [Internet]. Hoboken, NJ, USA: John Wiley & Sons, Inc.; 2003. Available from:  
27 <http://doi.wiley.com/10.1002/0471263397.env292>
- 28 66. Flemming H, Wingender J. The biofilm matrix. Nat Rev Microbiol [Internet].  
29 2010;8(9):623–33. Available from:



- 1 <http://dx.doi.org/10.1038/nrmicro2415%5Cnhttp://www.ncbi.nlm.nih.gov/pubmed/206761>  
2 45
- 3 67. Beech I, Hanjagsit L, Kalaji M, Neal AL, Zinkevich V. Chemical and structural  
4 characterization of exopolymers produced by *Pseudomonas* sp. NCIMB 2021 in  
5 continuous culture. *Microbiology*. 1999;145(6):1491–7.
- 6 68. Yang Y, Wikieł AJ, Dall’Agnol LT, Eloy P, Genet MJ, Moura JJG, et al. Proteins  
7 dominate in the surface layers formed on materials exposed to extracellular polymeric  
8 substances from bacterial cultures. *Biofouling* [Internet]. 2016;32(1):95–108. Available  
9 from: <http://www.tandfonline.com/doi/full/10.1080/08927014.2015.1114609>
- 10 69. Zaky A, Escobar I, Motlagh AM, Gruden C. Determining the influence of active cells and  
11 conditioning layer on early stage biofilm formation using cellulose acetate ultrafiltration  
12 membranes. *Desalination*. 2012;286:296–303.
- 13 70. Pasmore M, Todd P, Smith S, Baker D, Silverstein J, Coons D, et al. Effects of  
14 ultrafiltration membrane surface properties on *Pseudomonas aeruginosa* biofilm initiation  
15 for the purpose of reducing biofouling. *J Memb Sci* [Internet]. 2001 Nov;194(1):15–32.  
16 Available from: <http://linkinghub.elsevier.com/retrieve/pii/S0376738801004689>
- 17 71. Liu Y, Mi B. Effects of organic macromolecular conditioning on gypsum scaling of  
18 forward osmosis membranes. *J Memb Sci*. 2014;450:153–61.
- 19 72. Kochkodan V, Hilal N. A comprehensive review on surface modified polymer  
20 membranes for biofouling mitigation. *Desalination*. 2015. p. 187–207.
- 21 73. Suwarno SR, Hanada S, Chong TH, Goto S, Henmi M, Fane AG. The effect of different  
22 surface conditioning layers on bacterial adhesion on reverse osmosis membranes.  
23 *Desalination* [Internet]. Elsevier B.V.; 2016;387:1–13. Available from:  
24 <http://www.sciencedirect.com/science/article/pii/S0011916416300868>
- 25 74. Dufrene YF. Recent progress in the application of atomic force microscopy imaging and  
26 force spectroscopy to microbiology. *Curr Opin Microbiol*. 2003;6:317–23.
- 27 75. Abu-Lail NI, Camesano TA. Elasticity of *pseudomonas putida* KT2442 surface polymers  
28 probed with single-molecule force microscopy. *Langmuir*. 2002;18(10):4071–81.
- 29 76. Touhami A, Nysten B, Dufrière YF. Nanoscale mapping of the elasticity of microbial cells

- 1 by atomic force microscopy. *Langmuir*. 2003. p. 4539–43.
- 2 77. Bayer ME, Carlemalm E, Kellenberger E. Capsule of *Escherichia coli* K29:  
3 Ultrastructural preservation and immunoelectron microscopy. *J Bacteriol*.  
4 1985;162(3):985–91.
- 5 78. Bullitt E, Makowski L. Bacterial adhesion pili are heterologous assemblies of similar  
6 subunits. *Biophys J*. 1998;74(1):623–32.
- 7 79. Helenius J, Heisenberg C-P, Gaub HE, Muller DJ. Single-cell force spectroscopy. *J Cell*  
8 *Sci* [Internet]. 2008 May 6;121(11):1785–91. Available from:  
9 <http://jcs.biologists.org/cgi/doi/10.1242/jcs.030999>
- 10 80. Savage DC, Fletcher M, editors. *Bacterial Adhesion* [Internet]. Boston, MA: Springer US;  
11 1985. Available from: <http://link.springer.com/10.1007/978-1-4615-6514-7>
- 12 81. Williams V, Fletcher M. *Pseudomonas fluorescens* adhesion and transport through  
13 porous media are affected by lipopolysaccharide composition. *Appl Environ Microbiol*.  
14 1996;62(1):100–4.
- 15 82. Berne C, Ma X, Licata NA, Neves BRA, Setayeshgar S, Brun Y V., et al. Physiochemical  
16 properties of *caulobacter crescentus* holdfast: A localized bacterial adhesive. *J Phys*  
17 *Chem B*. 2013;117(36):10492–503.
- 18 83. Dupres V, Alsteens D, Andre G, Verbelen C, Dufrêne YF. Fishing single molecules on  
19 live cells. *Nano Today*. 2009. p. 262–8.
- 20 84. Engel A, Müller DJ. Observing single biomolecules at work with the atomic force  
21 microscope. *Nat Struct Biol*. 2000;7(9):715–8.
- 22 85. Engel A, Gaub HE, Müller DJ. Atomic force microscopy: A forceful way with single  
23 molecules. *Curr Biol*. 1999;9(4).
- 24 86. Fredrickson GH. The theory of polymer dynamics. *Curr Opin Solid State Mater Sci*.  
25 1996;1(6):812–6.
- 26 87. Flory PJ, Volkenstein M. Statistical mechanics of chain molecules. *Biopolymers*  
27 [Internet]. 1969;8(5):699–700. Available from:  
28 <http://doi.wiley.com/10.1002/bip.1969.360080514%5Cnpapers2://publication/doi/10.1002>  
29 [/bip.1969.360080514](http://doi.wiley.com/10.1002/bip.1969.360080514)

- 1 88. Sandal M, Valle F, Tessari I, Mammi S, Bergantino E, Musiani F, et al. Conformational  
2 equilibria in monomeric alpha-synuclein at the single-molecule level. *PLoS Biol.*  
3 2008;6(1):e6.
- 4 89. Dougan L, Li J, Badilla CL, Berne BJ, Fernandez JM. Single homopolypeptide chains  
5 collapse into mechanically rigid conformations. *Proc Natl Acad Sci U S A.*  
6 2009;106(31):12605–10.
- 7 90. Farrance OE, Paci E, Radford SE, Brockwell DJ. Extraction of Accurate Biomolecular  
8 Parameters from Single-Molecule Force Spectroscopy Experiments. *ACS Nano*  
9 [Internet]. 2015 Feb 24;9(2):1315–24. Available from:  
10 <http://pubs.acs.org/doi/abs/10.1021/nn505135d>
- 11 91. Friedlander RS, Vogel N, Aizenberg J. Role of Flagella in Adhesion of *Escherichia coli* to  
12 Abiotic Surfaces. *Langmuir.* 2015;31(22):6137–44.
- 13 92. Bowen WR, Hilal N, Lovitt RW, Wright CJ. Direct measurement of the force of adhesion  
14 of a single biological cell using an atomic force microscope. *Colloids Surfaces A*  
15 *Physicochem Eng Asp* [Internet]. 1998;136(1–2):231–4. Available from:  
16 <http://www.scopus.com/inward/record.url?eid=2-s2.0-0032580422&partnerID=tZOtx3y1>
- 17 93. Bowen WR, Lovitt RW, Wright CJ. Atomic force microscopy study of the adhesion of  
18 *Saccharomyces cerevisiae*. *J Colloid Interface Sci.* 2001;237(1):54–61.
- 19 94. Le DTL, Guérardel Y, Loubière P, Mercier-Bonin M, Dague E. Measuring Kinetic  
20 Dissociation/Association Constants Between *Lactococcus lactis* Bacteria and Mucins  
21 Using Living Cell Probes. *Biophys J* [Internet]. 2011 Dec;101(11):2843–53. Available  
22 from: <http://linkinghub.elsevier.com/retrieve/pii/S0006349511012562>
- 23 95. Ovchinnikova ES, Krom BP, van der Mei HC, Busscher HJ. Force microscopic and  
24 thermodynamic analysis of the adhesion between *Pseudomonas aeruginosa* and  
25 *Candida albicans*. *Soft Matter* [Internet]. 2012;8(24):6454. Available from:  
26 <http://xlink.rsc.org/?DOI=c2sm25100k>
- 27 96. Emerson IV RJ, Bergstrom TS, Liu Y, Soto ER, Brown CA, McGimpsey WG, et al.  
28 Microscale correlation between surface chemistry, texture, and the adhesive strength of  
29 *staphylococcus epidermidis*. *Langmuir.* 2006;22(26):11311–21.

- 1 97. Razatos A, Ong YL, Sharma MM, Georgiou G. Molecular determinants of bacterial  
2 adhesion monitored by atomic force microscopy. *Proc Natl Acad Sci U S A*.  
3 1998;95(19):11059–64.
- 4 98. Kang S, Elimelech M. Bioinspired single bacterial cell force spectroscopy. *Langmuir*.  
5 2009;25(17):9656–9.
- 6 99. Beaussart A, El-Kirat-Chatel S, Herman P, Alsteens D, Mahillon J, Hols P, et al. Single-  
7 cell force spectroscopy of probiotic bacteria. *Biophys J*. 2013;104(9):1886–92.
- 8 100. Diao M, Taran E, Mahler S, Nguyen TAH, Nguyen A V. Quantifying adhesion of  
9 acidophilic bioleaching bacteria to silica and pyrite by atomic force microscopy with a  
10 bacterial probe. *Colloids Surfaces B Biointerfaces*. 2014;115:229–36.
- 11 101. Beaussart A, El-Kirat-Chatel S. Quantifying the forces guiding microbial cell adhesion  
12 using single-cell force spectroscopy. *Nat Protoc [Internet]*. 2014;9(5):1049–55. Available  
13 from:  
14 <http://www.ncbi.nlm.nih.gov/pubmed/24722404>  
15 <http://www.nature.com/nprot/journal/v9/n5/abs/nprot.2014.066.html>
- 16 102. Rodriguez-Emmenegger C, Janel S, de los Santos Pereira A, Bruns M, Lafont F.  
17 Quantifying bacterial adhesion on antifouling polymer brushes via single-cell force  
18 spectroscopy. *Polym Chem [Internet]*. 2015;6(31):5740–51. Available from:  
19 <http://xlink.rsc.org/?DOI=C5PY00197H>
- 20 103. Aguayo S, Strange A, Gadegaard N, Dalby MJ, Bozec L. Influence of biomaterial  
21 nanotopography on the adhesive and elastic properties of *Staphylococcus aureus* cells.  
22 *RSC Adv [Internet]*. 2016;6(92):89347–55. Available from:  
23 <http://xlink.rsc.org/?DOI=C6RA12504B>

24  
25

26 **Figure legends**

27 **Figure 1. Schematic representation of the Atomic Force Microscope.**

28 **Figure 2. AFM images of bioprocess engineering surfaces** (A) Cyclopore microfiltration  
29 membrane (3.2 $\mu\text{m}^2$ ) (B) Humic acid layer fouling an ultrafiltration membrane (3.5 $\mu\text{m}^2$ ) (C) Air  
30 bubbles at a membrane surface (0.75 $\mu\text{m}^2$ ) (D) Stainless steel process plant surface.  
31 (10 $\mu\text{m}^2$ ). (E) Lawn of *Saccharomyces cerevisiae* cells (brewing yeast NCYC 1681) showing

1 budding scars ( $15 \mu\text{m}^2$ ) (F) *Shewanella oneidensis* cell showing protein clusters at surface  
2 formed during anaerobic respiration and microbial fuel cell operation ( $1.2\mu\text{m}^2$ )

3  
4 **Figure 3. AFM Force spectroscopy curve of a single *S.cerevisiae* cell (stationary phase)**  
5 **with freshly cleaved mica in  $10^{-2}$  M NaCl pH 5.0.**

6  
7  
8 **Figure 4. SEM image of a cell probe A) *Saccharomyces cerevisiae* B) *Aspergillus***  
9 ***niger***

10

11

12

1  
2  
3  
4  
5  
6  
7  
8  
9  
10  
11  
12  
13  
14  
15  
16